Hydrology
Current Research
ISSN: 2157-7587

Ngaina and Opere, Hydrol Current Res 2017, 8:4
DOI: 10.4172/2157-7587.1000285

Research Article OMICS International

Hydrological Characteristics of Lower Nzoia Sub-basin in Kenya

Ngaina JN[1,2*] and Opere AO[2]

[1]Department of Meteorology, South Eastern Kenya University, PO Box 170-90200, Kitui, Kenya
[2]Department of Meteorology, University of Nairobi, PO Box 301975-00100, Nairobi, Kenya

Abstract

This study sought to investigate hydrological characteristics of lower Nzoia sub-basin in Kenya. Trend (long and medium) utilized graphical and statistical approach. Extreme value (EV) analysis based on frequency, annual maximum flows, exceedance probability, low flows and probable maximum precipitation was used. Quality control showed consistency in rainfall, temperature and discharge datasets. Maximum-minimum monthly and annual flows and rainfall showed maximum flows centered in March-to-May (peak) with increasing temperature. Trends, seasonality and cycles were identified and maximum values in rainfall and discharge closely followed the pattern for peak rainfall seasons. Based on the flow magnitudes and 100-year return period, the upstream station (1EE01) had lower values compared to downstream station (1EF01) for different assumed distributions and thus 1EF01 assumed to be more reliable. Exponential and Pareto distributions indicated a normal tail and thus appropriateness of EV1/Gumbel distribution in calibrating AM series. Best conventional calibration results based on assumed distributions using EV1/Gumbel superimposed with the extreme value distribution fitted along with the exponential/Pareto Q-Q plots for comparison. Estimated maximum withdrawal in monthly terms for 1EE01 and 1EF01 was 262.5 and 368.4 cumecs respectively. Analyses of low stream flow indicate probable availability of water in streams at different return periods.

Keywords: Exceedance probability; Extreme value analysis; Q-Q plot return period; Trend analysis; Annual maximum series; Probable maximum precipitation

Introduction

Water availability and its use form fundamental components for economic, social and cultural development in Kenya [1]. Kenya's record of flood disasters indicates the worst floods that were recorded in 1961-62 and 1997-98 are associated with a dipole reversal in atmospheric circulation (Indian Ocean Dipole) and Indian Ocean sea surface temperatures [2]. This event caused widespread flooding, rapid and prolonged increases in the levels of many lakes in East Africa and significant economic disruption [3]. River flow is a variable of most direct practical importance in hydrology. Hydrological extremes such as floods and droughts have always been a major societal concern with flood losses continuing to rise, soaring to tens of billions of dollars (US) in material damage and to thousands of flood fatalities a year [4].

Several distribution types are used to model extremes in hydrology, but the merits of their applicability to different types of data and for different purposes have not been clearly established [5] due to use of a particular distribution in any country being subjective. Although many studies on the choice of distribution exist [6-8] observed that the treatment of choice of distribution and parameter estimation separately is not justified. Chow et al. [9-11] provided a comprehensive review of studies that compared various probability distributions and parameter estimator procedures for fitting low stream flow series. For example, United States Geological Survey (USGS) uses a LP3 distribution to describe annual minimum stream flow series [12-14] while the National Drought Atlas developed for U.S uses a Generalized Wakeby distribution to describe annual minimum stream flow series [15]. Hosking et al. [16] used the Annual Maxima Series (AMS) and [17] used the Peaks over Threshold (PoT) method. In East Africa, Mkhandi et al. [18] carried out a comparison between the annual maximum and peaks over threshold models for flood frequency distributions. Flood frequency analyses studies have also been carried out using of annual maxima series in the Nile equatorial basin [19] and Lake Victoria basin [20].

Although nonstructural measure such as flood forecasting with sufficient lead-time [21,22] and structural measures such as building larger structures could be used for flood hazard mitigation and for minimizing flood related losses, the risk of flood hazards due to their extremely low probability cannot be completely circumvented. Assessment of potential flood damages requires information on hydrology (maximum discharge, water levels), the use of floodplains, and loss functions for each category of economic activities on areas exposed to the risk of floods. Therefore, the goal of this study is to examine the hydrological characteristics of Lower Nzoia, a sub catchment of the Lake Victoria region using observed and simulated data with particular emphasis on flood frequency analysis. The knowledge of magnitude-frequency relationships can then be used in the design of dams, spillway of dams, highway, bridges, culverts, water supply systems and flood control structures.

Study Area, Data and Model

Study area

The lower Nzoia sub-basin lies within the Nzoia sub-basin of the Lake Victoria basin located at latitudes 34°-36°E and longitudes 0°03-

***Corresponding author:** Joshua Ndiwa Ngaina, Department of Meteorology, South Eastern Kenya University, PO Box 170-90200, Kitui, Kenya and Department of Meteorology, University of Nairobi, PO Box 301975-00100, Nairobi, Kenya, Tel: +254726792701; E-mail: jngaina@seku.ac.ke

Received September 01, 2017; **Accepted** September 22, 2017; **Published** September 30, 2017

Citation: Ngaina JN, Opere AO (2017) Hydrological Characteristics of Lower Nzoia Sub-basin in Kenya. Hydrol Current Res 8: 285. doi: 10.4172/2157-7587.1000285

1°15′ N in Kenya [21] as shown in Figure 1. It drains into the Lake Victoria and Nile river basins. Lake Victoria, with an area of 68,600 km^2, is the second largest freshwater lake in the world 24. The Nzoia sub-basin covers approximately 12,900 km^2 of area with an elevation ranging between 1100 to 3000m. The Nzoia River originates in the southern part of the Mt. Elgon and Western slopes of Cherangani Hills [23]. The lowlands are characterized by predominant clayey soils at 77% [24]. Nzoia, a sub-basin of Lake Victoria, is chosen as the study area because of its regional importance as it is a flood-prone basin and also one of the major tributaries to Lake Victoria [24].

Data and methodology

Daily rainfall and temperature was sourced from the Kenya Meteorological Department (Table 1) while daily discharge (Table 2) was sourced from Kenya Water Resources Management Authority. Rainfall runoff modeling was used to extend the data series and fill in for missing data before subjecting to extreme value analysis. Data quality control and homogeneity testing also included arithmetic mean and single mass curve respectively. The rainfall-runoff modeling was carried out using the Australian Water Balance Model (AWBM), which is part of the Rainfall-Runoff Library (RRL) package. The model generates catchment runoff from rainfall and potential evaporation. The main inputs to this model are observed evaporation, rainfall, and river flow measurements, in this case with a daily time step (although the model can use hourly data if available). The AWBM is a catchment water balance model that relates runoff to rainfall, and calculates losses from rainfall for flood hydrograph modelling. The model uses three surface stores to simulate partial areas of runoff. The water balance of each surface store is calculated independently of the others. The model calculates the moisture balance of each partial area at either daily or hourly time steps. At each time step, rainfall is added to each of the three surface moisture stores and evapotranspiration is subtracted from each store. The water balance equation is:

$$Store = store_n + rain - evap \ (n=1 \text{ to } 3) \quad (1)$$

If the evapotranspiration demand exceeds the available moisture, the value of moisture in the store is set to zero. If the value of moisture in the store exceeds the capacity of the store, the excess becomes runoff and the store is reset to its capacity. When runoff occurs from any store, part of the runoff becomes recharge of the base flow store if there is base flow in the stream flow. Daily discharge data for station 1EE01 (Rwambwa), covering the period 1/1/2001 to 19/5/2013 was used. The calibration period was 1/1/2001 to 31/10/2010 while the verification period is 1/11/2010 to 31/12/2012. The daily rainfall data for Bunyala station and data on seasonal average evaporation over the same period were also used.

Trend (long and medium term) utilized both graphical (time series plots) and statistical approach. The principle in statistical approach is to test, statistically, whether or not the two means are statistically different from each other with any significant shift in the mean an indication of a changing trend. This difference in the two means is then compared against the standard error of estimate (S_E). Statistical technique involves computation of the t-statistic and using the t-distribution table, the $t_{tabulated}$ value at 5% significance level and N_2 degrees of freedom is determined and compared with the t-computed. If the $t_{computed}$ is less than the $t_{tabulated}$, the 'null hypothesis' that there was no significant

	Station Name	Station Number	Co-ordinates	Record period
1	Bungoma water supply station	8934134	0 35N 34 34E	1970-2001
2	Kitale meteorological station	8834098	1 00N 34 59E	1970-1975
3	Bunyala irrigation scheme	8834139	0 05N 34 03E	1970-2001
4	Kimilili agricultural department	8934061	0 27N 34 51E	1970-2001
5	Soil conservation service, Eldoret	8935102	0 34N 35 18E	1970-2001
6	Chorlim ADC Station	8834013	1 02N 34 48E	1970-2001

Table 1: Rainfall stations.

	Station ID	Location	Location
1	1EE01	0.18 N, 34.22 E	Nzoia
2	1EF01	0.12 N, 34.09 E	Nzoia

Table 2: Comparative statistics for runoff.

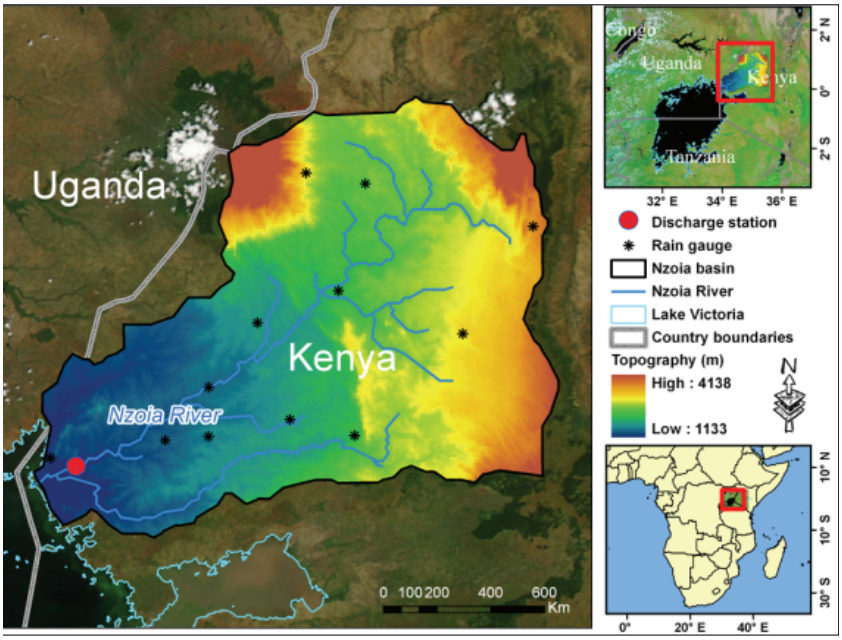

Figure 1: Map of Nzoia river basin in Lake Victoria region [24].

difference between the means is accepted. Conversely, if the $t_{computed}$ is greater than $t_{tabulated}$, the 'null hypothesis' is rejected and the 'alternative hypothesis' is accepted which means that the two means are statistically different.

The long-term trend analysis was applied to the discharge, precipitation and temperature data, which were divided into two 12-year periods: 1976 to 1988 (Period 1) and 1989 to 2001 (Period 2). The medium-term trend analysis was used to analyze the variation of flow levels over a period of 10 years (1992 to 2001), with this period divided into two sub-periods: 1992 to 1996 (Period 1) and 1997 to 2001 (Period 2).

Extreme value analysis was then used to determine the return period of extreme events. In fitting extreme value distributions, parameters were estimated by the Method of Moments (MOM), the Maximum Likelihood (ML) method or the method of Probability Weighted Moments (PWM). The probability density functions of the family of extreme value distributions are given by:

$$F(\mathrm{x}) = \exp\left(-\exp-\left(\frac{x-a}{\beta}\right)\right) if\, \gamma = 03 \quad (2)$$

$$F(\mathrm{x}) = \exp\left(-\exp-\left(\frac{x-a}{\beta}\right)\right) if\, \gamma = 03 \quad (3)$$

where γ, α, and β are the shape parameter (extreme value function), threshold value and scale parameter respectively. For γ=0, the distribution is a Gumbel or Extreme Value Type I (EV1) distribution and for γ>0, the distribution is a Fretchet of EV2 while for γ<0, the distribution is a Weibull or EV3.

Exponential and Pareto Quantiles-quantile (Q-Q) plots were used to test goodness of fit in the selection of a distribution to model extreme events and included. Estimating the parameters of the distributions was done from the slope of the Q-Q plots after an optimum threshold had been chosen. The optimal threshold rank was chosen at a position where the extreme value index had little variance and the Mean Square Error (MSE) was minimum. The extreme value index corresponding to the optimal threshold rank gave the value of γ, while β and α were then generated automatically. For a normal tail distribution, the optimal threshold rank in the Exponential Q-Q plot was also selected at a point where the slope was more stable and the MSE was minimized. The value of the slope corresponding to the optimal threshold rank gave the value of β, while α was automatically generated. Calculation of Return period discharges was achieved using parameters obtained in the distribution that corresponded to the tails using the equation 4.

$$T\ (number\ of\ years) = F(\gamma, \beta, \alpha) \quad (4)$$

The parameters obtained from the Q-Q plots were used in the extreme value distribution equations using specified values of T. The results were the discharges corresponding to each return period for each gauging site. To indicate the time the river discharge was exceeded, flow duration curves which was represented by empirical exceedance frequency was computed. Low flow frequency analysis was used to extract low stream flows from discharge series. Low flows are constructed from a series of annual minima, with the available stream flow data being extrapolated by a theoretical distribution to improve the accuracy of the estimation. The annual minimum values were transformed into high values by using $X=1/x$ and these transformed (high) values then sorted in descending order of magnitude and the recurrence interval calculated. For the probability distribution of the extremes below a threshold x_t in n period of years, the return period, T, of low stream flows was calibrated by using the following equation:

$$T_c = \frac{n}{t} * \left[\frac{1}{\exp\left(-\left(\frac{x^{-1} - x_t^{-1}}{\beta}\right)\right)}\right] \quad (5)$$

Where T_c is the calibrated return period in years based on the exponential Extreme Value distribution and β the extreme value parameter. The design stream flow for a certain return period was estimated on the basis of linear regressions in the exponential quantile plots.

$$X_T = x_t^{-1} + \beta\left(In(\mathrm{T}) - \mathrm{In}\left(\frac{n}{t}\right)\right)\ 6 \quad (6)$$

Where X_T is the estimated design low stream flow at the return period T years, x_t is the threshold value below which all stream flow are low flows, 'n' is the years of record, and t is the number of extracted low stream flows.

Probable Maximum Precipitation (PMP) values were calculated using the statistical Hershfield method, which is based on Chow's general frequency equation. Using precipitation records for all the stations in consideration, annual and monthly maximum values for each station were extracted and the values sorted in ascending order; the values of $\bar{X}_n$, $\bar{X}_{n-1}$, σ_n and σ_{n-1} were calculated; the frequency factor K_m was also determined for the station and the PMP values were then calculated for each of the stations using the corresponding K_m values obtained.

Results and Discussion

Data quality control

Analysis of rainfall-runoff modeling was based on comparative and Univariate statistics as shown in Table 3. Table 3 therefore provided a statistical comparison between observed and simulation runoff for the calibration and validation period, with the results indicating a fairly good fit. It is important to note that the y-axis (runoff values) have been log transformed.

Figure 2 presents the observed and generated hydrograph between November 2010 and July 2012 inclusive. Although higher flows are simulated with more accuracy than lower flows, nevertheless maximum runoff values derived from the model at this timescale will not be representative since individual floods are caused by episodic rainfall events.

Analysis of rainfall-runoff modeling based on comparative and Univariate statistics provided a statistical comparison between observed and simulated runoff for the calibration and validation period, with the results indicating a fairly good fit. Single mass curves for all rainfall and discharge stations were straight lines with the coefficient of determination (R^2) being a value that is close to 1, an indicator of consistent and of sufficient quality. At station 1EE01, the maximum flow of 596 m^3/s was recorded on 3/5/1963, and the minimum flow of 0.07 m^3/s was recorded on 26/3/1981. The mean daily flow for this location was 90.62 m^3/s with a standard deviation of about 63 m^3/s. For station 1EF01, the maximum flow of 931 m^3/s recorded on 26/11/1977, and the minimum flow of 5.84 m^3/s recorded on 25/2/1975. The mean daily flow for this location was 144.4 m^3/s with a standard deviation of about 103 m^3/s. Maximum and minimum monthly and annual flows

Comparative statistics for runoff								
Variable	**Start**	**End**	**Length**		**Relative Difference**	**Absolute Difference**	**Nash-Sutcliffe**	**Correlation**
Calibration	12/31/2002	10/31/2010	2862		0.81%	22.663	0.642	0.802
Verification R	12/31/2011	7/31/2012	214		4.00%	9.575	0.802	0.928
Univariate Statistics								
Variable	**Start**	**End**	**Length**	**Missing**	**Total (mm)**	**Mean (mm)**	**Std.Dev. (mm)**	**Skew (mm)**
Calib. Observ	12/31/2002	10/31/2010	2862	0	2795.047	0.977	0.721	0.866
Verif. Observ	12/31/2011	7/31/2012	214	0	239.253	1.118	0.846	0.412
Runoff	12/31/2002	10/31/2010	2862	0	2817.71	0.985	0.551	0.91
Runoff (Verif)	12/31/2011	7/31/2012	214	0	248.827	1.163	0.584	0.103

Table 3: Comparative statistics for runoff.

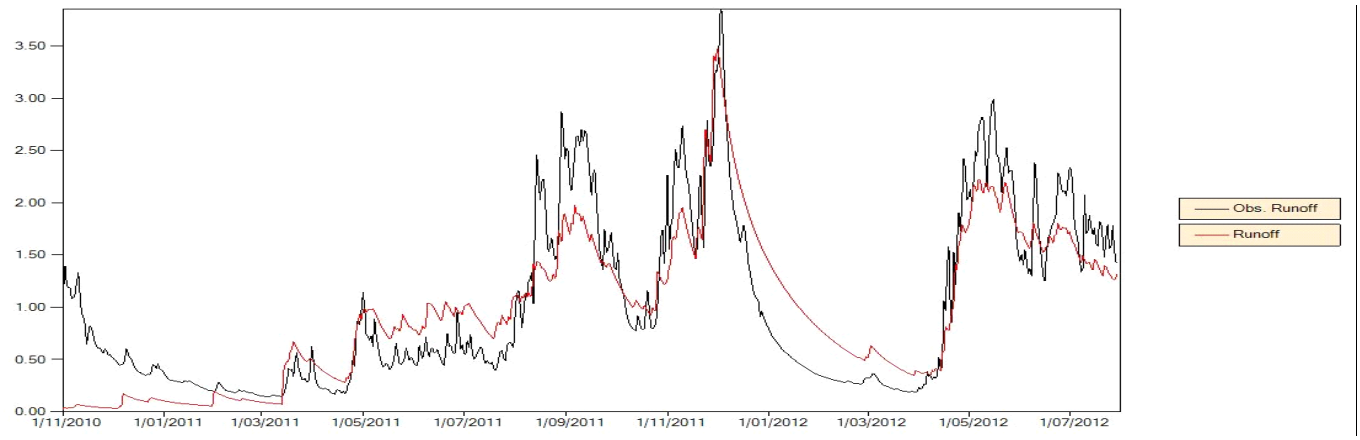

Figure 2: Observed and simulated runoff hydrograph.

derived from the generated box plots showed maximum flows centred in the months of March to May (peak rainfall season). For rainfall stations, results from Chorlima ADC rainfall station (8834013) gave a maximum daily rainfall of 100.6 mm and a minimum daily rainfall of 0.0 mm. The mean daily rainfall for this location was 3.4 mm, with a standard deviation of about 6.8 mm. The maximum, minimum, monthly and annual rainfalls derived from the generated box plots showed maximum rainfall centered in the months of March to May. Data inconsistencies were investigated using mass curves, and the results showed consistency in both the rainfall and discharge records.

Trend analysis

Rainfall: Graphical plots of the observations for all the rainfall stations for the period 1970 to date showed a slight increasing trend for all stations except Eldoret Soil Conservation Service Station, which had a slight decreasing trend and Bungoma Water Supply which had no trend at all. The implication of decreasing trends in rainfall is a signal of climate change and could pose future challenges in water resources available and access in the basin whereas the opposite would bring with it challenges of dealing with flood disasters including landslides. Based on long term sample means (Table 4), the rainfall records showed that the two-sample means were not different. However, a test of significance using t statistic indicated that for all rainfall stations except Bungoma water supply station, the two means were not different in the long-term and thus presence of significant trend. Based on the medium-term sample means (Table 5), the results indicated a significant medium-term trend, which meant that the values were either increasing or decreasing. The trends, seasonality and cycles in the series were identified and maximum values in rainfall and discharge were noted to closely follow the pattern for peak rainfall seasons.

Figure 3 shows the average monthly rainfall for all the stations considered in the basin, depicting the seasonal trends. Bungoma water supply indicated that there was a major peak in rainfall in April and decreased gradually towards August-September and then slightly increasing to a minor peak in October, after which there is a decrease in the total monthly rainfall up to a minimum in December and January and then an increase to begin the cycle again. The average monthly rainfall for Kimilili agricultural department shows a major peak in May which decreases up to July and then increases to a minor peak in October, then a decrease which results to January having the least total monthly rainfall. Bunyala irrigation scheme showed a major peak in May with monthly rainfall reducing the following month of July, then increases throughout the season until another major peak is reached in May. From the Soil Conservation service, Eldoret, it was observed that a minor peak was observed in April with rainfall reducing over the following month of May and then increases afterwards until a major peak is reached in July. The month with the least rainfall is December and January. Kitale meteorological station indicated that the region experiences a major peak in May after which monthly rainfall gradually decreases with a minor peak in July and August. From then, the monthly rainfall continues to decrease until a minimum is reached in December and January for the next cycle to begin (Table 6).

Discharge: The annual variation of discharge at the two gauging stations 1EE01 and 1EF01 is shown in Figure 4. The peak discharges can be seen during the months of April to June and August to October, with the higher peaks in the second of those periods (which coincides with the short rains period). The time series of flows indicated a decreasing trend over station 1EE01 and an increasing trend over

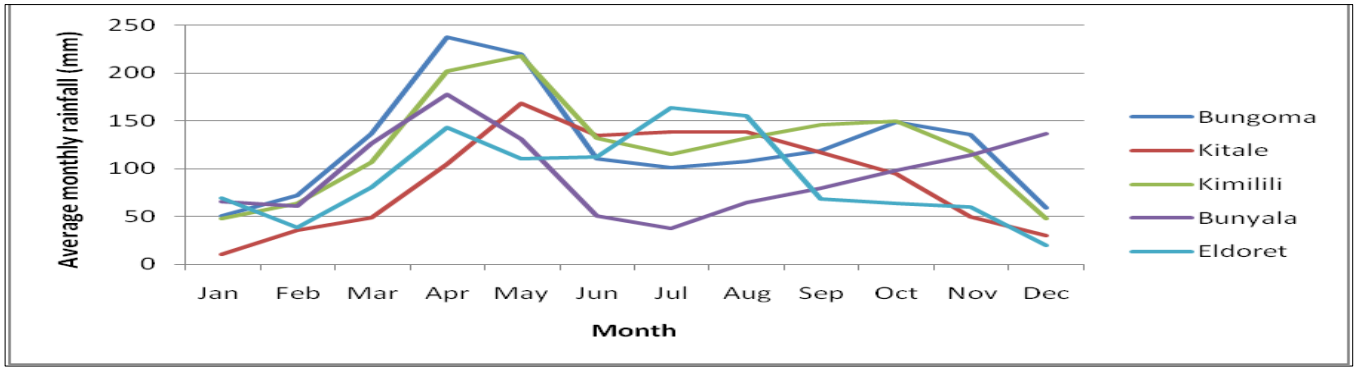

Figure 3: Average monthly rainfall for the rainfall stations.

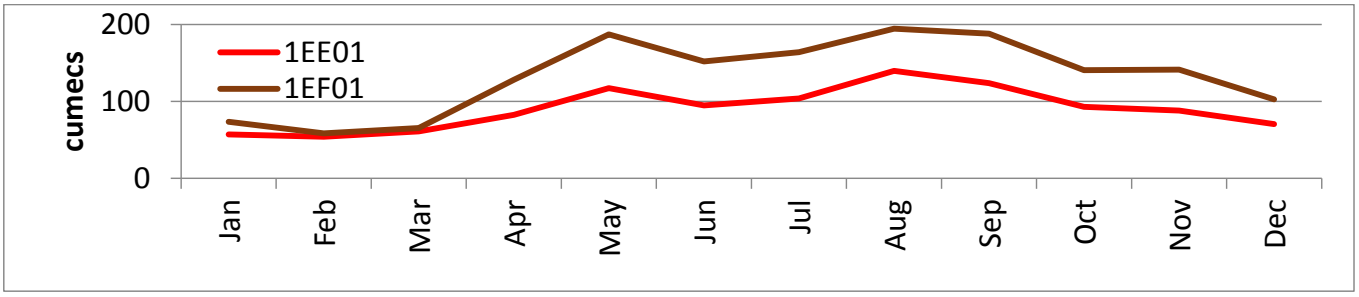

Figure 4: Annual variation of discharges at gauging stations 1EE01 and 1EF01.

Station	sample means					t-statistic		
	X_1	X_2	$\|X_1-X_2\|$	S_E	Conclusion	t-computed	t-tabulated (α=0.05)	Conclusion
Bungoma water supply	159	113	46.8	9	significant trend	5.82	1.97	significant trend
Kitale meteorological	105	104	0.7	8	significant trend	0.108	1.97	no significant trend
Bunyala irrigation scheme	81.9	93.5	11.6	8	significant trend	-1.83	1.97	no significant trend
Kimilili Agricultural Department	122	123	1.23	9	significant trend	0.43	1.97	no significant trend
Eldoret soil conservation service	84.9	82.8	2.1	8	significant trend	0.32	1.97	no significant trend

Table 4: Long term Statistical trend analysis of rainfall.

Station	Based on Sample means					Based on t-statistic		
	X_1	X_2	$\|X_1-X_2\|$	S_E	Conclusion	t-computed	t-tabulated (α=0.05)	Conclusion
Bungoma water supply	131.7	96.7	35.1	12.7	significant trend	2.88	2.00	significant trend
Kitale meteorological	101.7	106.7	5.08	12.2	significant trend	-0.53	2.00	significant trend
Bunyala irrigation scheme	95.2	91.1	4.17	13.7	significant trend	0.39	2.00	significant trend
Kimilili agricultural department	122.0	131.5	9.55	8.1	significant trend	-0.832	2.00	significant trend
Soil conservation service, Eldoret	76.8	90.8	14.05	13.4	no significant trend	-1.48	2.00	significant trend

Table 5: Medium term trend analysis of rainfall.

Station	Based on sample means					Based on t-statistic		
	X_1	X_2	$\|X_1-X_2\|$	S_E	Conclusion	t-computed	t-tabulated (α=0.05)	Conclusion
1EF01	122.5	145.4	22.9	9.8	significant trend	-2.91	1.97	no significant trend
1EE01	87.7	85.1	2.6	5.2	significant trend	0.69	1.97	no significant trend

Table 6: Long term trend analysis of discharge.

1EF01 (Rwambwa) station (Figure 4). However, only 1.9% of data were noted to fit into the trend line over station 1EE01 compared to 6.9% of data which fitted into the trend line for station 1EF01.

Temperature: Graphical plots of time series analysis for the mean annual temperature observed at Kitale and Eldoret station from the years 1991 to 2010 as shown in Figure 5a and 5b respectively indicates an increasing trend with only 20.6% of maximum and minimum temperature data fitting the linear regression line in Kitale station while 13.8% of minimum temperature and 1.8% of maximum temperature fitted the linear regression line in Eldoret (Table 7).

Extreme value analysis:

Frequency analysis: Several extreme value distributions have been tested using the IH Floods toolkit. The results of the distribution fit for discharge are presented for various methods of parameter estimation as generated from the daily discharge records in Table 8. From the flood frequency curves derived from daily values (Figure 6), it is noted that the Gumbel (EV1) family of distributions fit the data reasonably well, and are considered most stable and suitable over the lower Nzoia sub-basin. Based on the flow magnitudes and 100-year return period, the upstream station (1EE01) was noted to have lower values compared to downstream station (1EF01) for different assumed distributions. The study notes that the flow magnitudes from the upstream station for the 100-year return period estimated at 633.6 cumecs differed significantly with flow magnitudes values found by a study on the National water master plan of the republic of Kenya report in 1992 which estimated the value at 801 cumecs. However, a recent study on the national water master plan (2013) for the republic of Kenya by the Japanese government indicates that flow magnitude values at the downstream station (1EF01) of 1,075 cumecs were comparable to flow magnitude values of 1151.7 cumecs found in this study. Therefore, the flow magnitude values at the downstream station (1EF01) were assumed to be more reliable compared to upstream station.

Annual maximum flows: The analysis using Quantile-Quantile (Q-Q) plots was done on the annual maximum flow values obtained from monthly average flow records for each station. The results of the Exponential and Pareto distributions for the two locations indicate a normal tail, suggesting that the EV1/Gumbel distribution would be an appropriate statistical distribution to calibrate the AM series for the stations. The best conventional calibration results (considering MOM, MLE and PWM calibration) using the EV1/Gumbel superimposed with the extreme value distribution fits along with the exponential/Pareto Q-Q plots for comparison purposes, and is shown in Figures 7-10 for a normal tail distribution fit. The estimated parameters from the Q-Q plots, based on annual maximum values from daily observations for the two stations are presented in Table 9.

Exceedance probability and flow magnitude: A summary exceedance probability and flow magnitudes is presented in Tables 10 and 11 for daily and monthly flow data respectively. The flow duration curves and exceedance probability corresponding to flow data are presented in Figures 11 and 12.

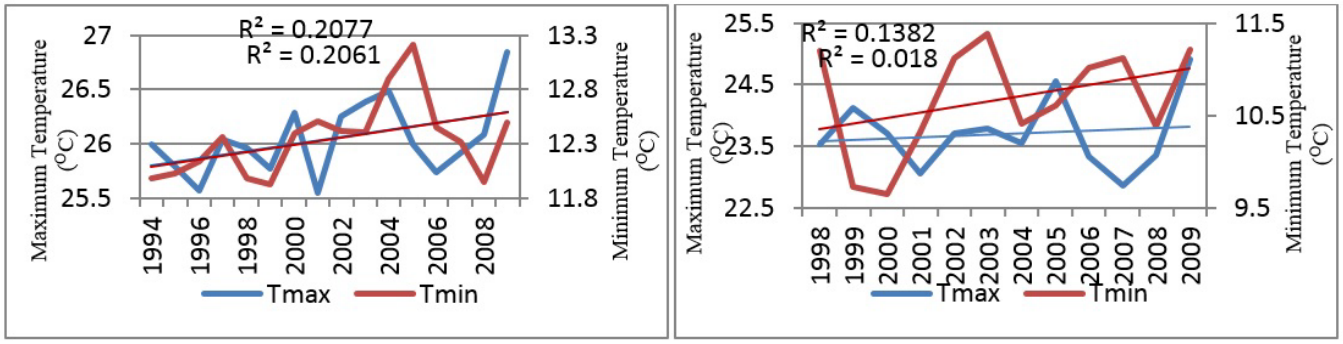

Figure 5: Time series of Maximum and minimum temperature over a) Kitale and b) Eldoret Station.

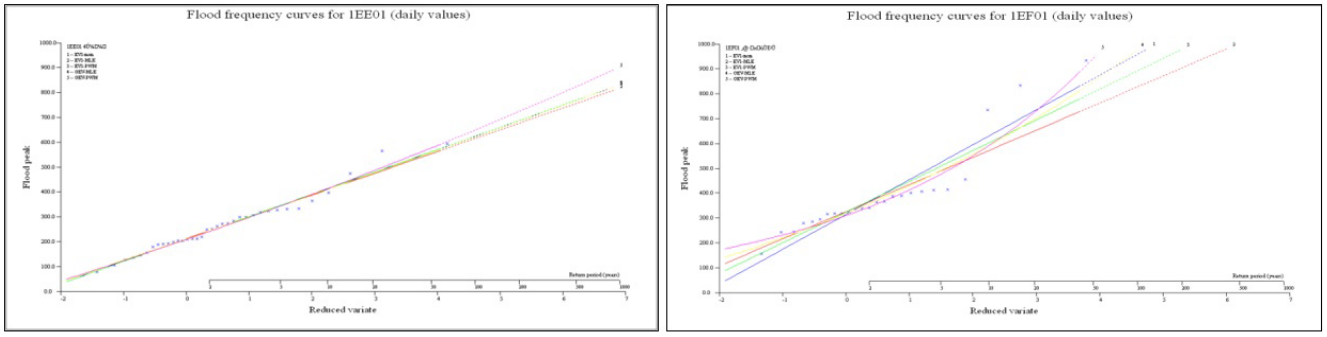

Figure 6: Flood frequency curves for a) 1EE01 b) 1EF01 derived from daily values.

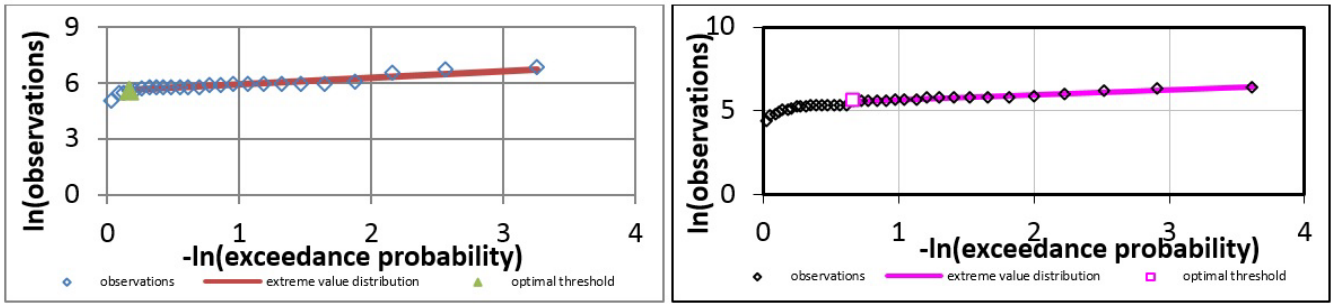

Figure 7: Pareto Q-Q Plot of Annual Maximum Flows at a) 1EF01 and b) 1EE01.

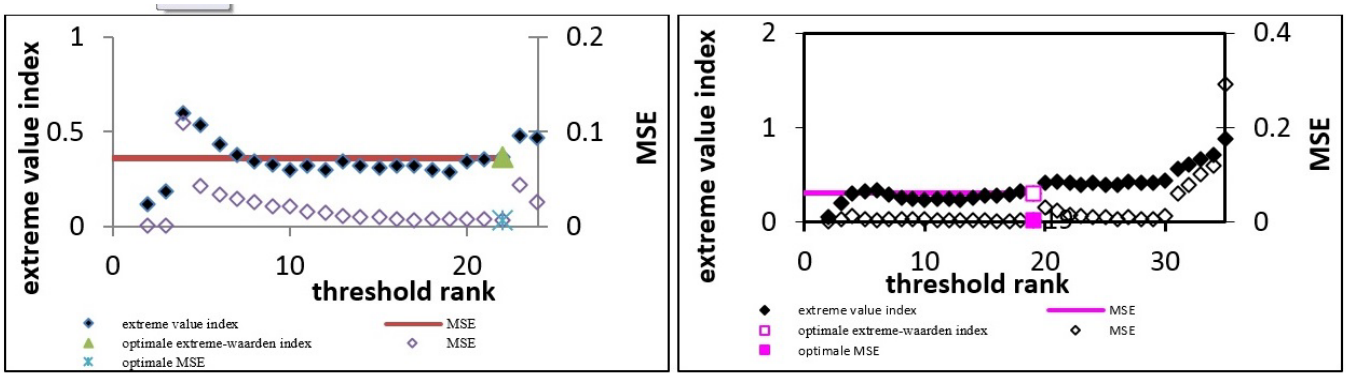

Figure 8: Slope Pareto Q-Q plot for a) 1EF01 and b) 1EE01.

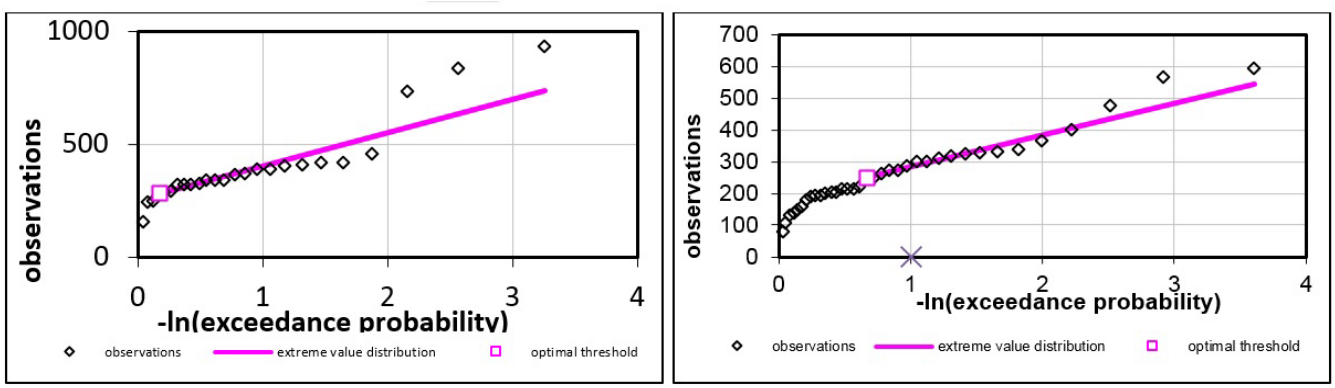

Figure 9: Exponential Q-Q Plot of Annual Maximum Flows at a) 1EF01 and b) 1EE01.

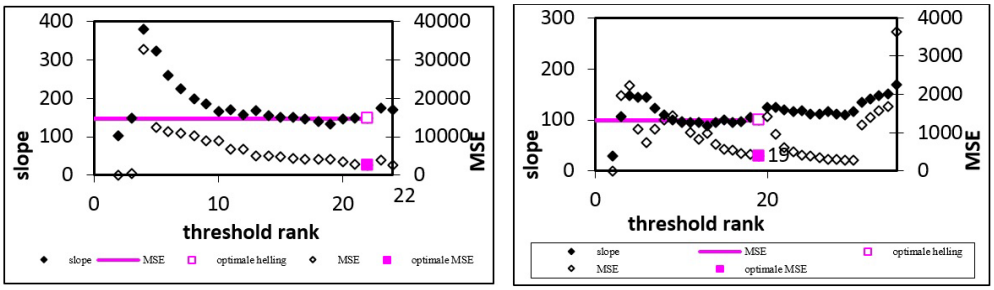

Figure 10: Slope exponential Q-Q plot for a) 1EF01 and b) 1EE01

Station	Based on sample means					Based on t-statistic		
	X_1	X_2	$\|X_1-X_2\|$	S_E	Conclusion	t-computed	t-tabulated (α=0.05)	Conclusion
1EF01	160.5	147.3	13.2	14.1	no significant trend	1.19	2	no significant trend
1EE01	85	84.9	0.1	5.6	significant trend	0.04	2	no significant trend

Table 7: Medium term trend analysis of discharge.

Station	Return periods									
	2	5	25	50	100	250	500	700	900	1000
1EE01	EV1-Mom (u=213.008 a=89.726)									
	245.9	347.6	500	563.1	625.8	688.2	770.5	800.8	823.3	832.8
	EV1-MLE (u=214.006 a=97.617)									
	246.1	345.4	494.3	555.9	619.2	697.6	758.4	787.9	810	830.5
	EV1-PWM (u=212.935 a=89.851)									
	245.9	347.7	500.3	563.5	633.6	708.9	771.2	801.5	824.1	850.3
	GEV-MLE (u=213.642 a=87.412 k=-0.0077)									
	245.7	345.5	496.7	559.9	633.7	706.5	770	800.9	824	851.1
	GEV-PWM (u=210.909 a=87.105 k=-0.0403)									
	243.1	345.6	508.3	579	704.7	749.4	826	864	892.6	890.5
1EF01	EV1-Mom (u=316.322 a=140.189)									
	367.7	526.6	764.7	863.3	961.2	1090.1	1187.4	1234.6	1269.9	1284.7
	EV1-MLE (u=327.513 a=109.242)									
	367.6	491.4	676.9	753.8	830	930.5	1006.3	1043.1	1070.6	1082.1
	EV1-PWM (u=325.892 a=123.609)									
	371.2	511.3	721.3	808.2	894.5	1008.1	1094	1135.6	1166.7	1179.7
	GEV-MLE (u=319.977 a=104.425 k=-0.1311)									
	359.2	493.1	734.9	851.9	979.3	1165.7	1322.2	1403.4	1466.4	1493.4
	GEV-PWM (u=311.556 a=89.933 k=-0.2786)									
	346.3	479	775.7	946.1	1151.7	1491.2	1811.8	1991.2	2136.5	2200.6

Note: u and a represents scale and location parameters for the respective distributions

Table 8: Flow Magnitudes and Return Periods for Different Assumed Distributions.

Station code	Parameters		
	Gamma	Beta	Alpha
1EF01	0.3623	101.8296	281.042
1EE01	0.3038	76.0294	250.205

Table 9: Estimated parameters from the Q-Q plots.

Exceedance probability of flow	1EE01 (M^3/S)	1EF01 (M^3/S)
Q_{80}	205.87	289.24
Q_{85}	199.82	280.29
Q_{90}	194.12	271.85
Q_{95}	188.72	263.87

Table 10: Exceedance probability and flow magnitudes.

	1EE01 (Upstream)			1EF01 (Downstream)		
Month	Q85 flow	Q90 flow	Q95 flow	Q85 flow	Q90 flow	Q95 flow
January	184.21	186.03	188.21	302.14	305.45	309.41
February	174.67	176.49	178.68	242.42	245.07	248.24
March	167.33	168.6	170.11	316.83	320.52	324.96
April	362.13	365.72	370.05	321.12	323.52	326.41
May	315.58	318.44	321.88	449.11	452.85	457.34
June	201.32	202.8	204.59	310.14	312.15	314.56
July	207.65	209.02	210.66	392.33	395.56	399.44
August	301.22	303.15	305.47	575.98	581.43	587.98
September	326.21	328.95	332.25	591.64	597.41	604.33
October	248.59	250.75	253.34	479.83	484.69	490.53
November	213.71	215.43	217.48	474.42	479.13	484.79
December	188.45	190.02	191.9	392.6	396.75	401.74

Table 11: Exceedance probability for monthly average flows.

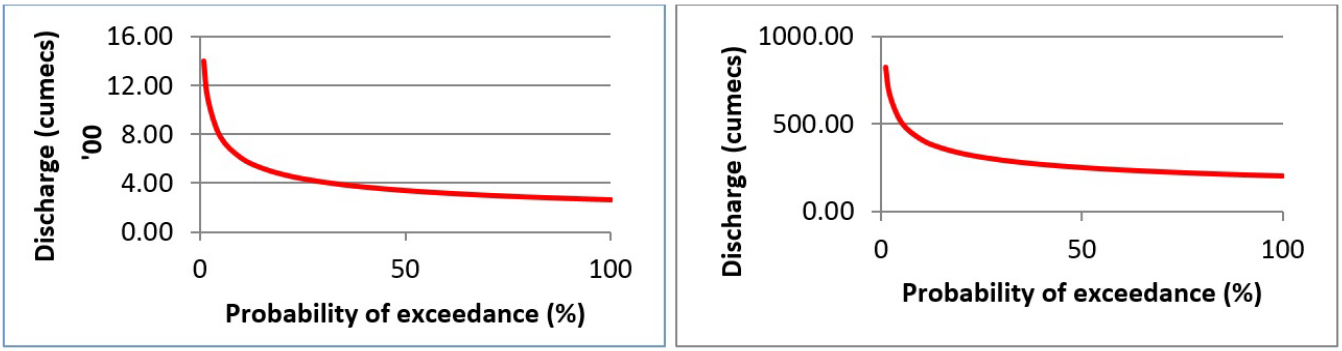

Figure 11: Monthly average Flow duration curve for a) 1EF01 (GPD) b) 1EE01 (GPD).

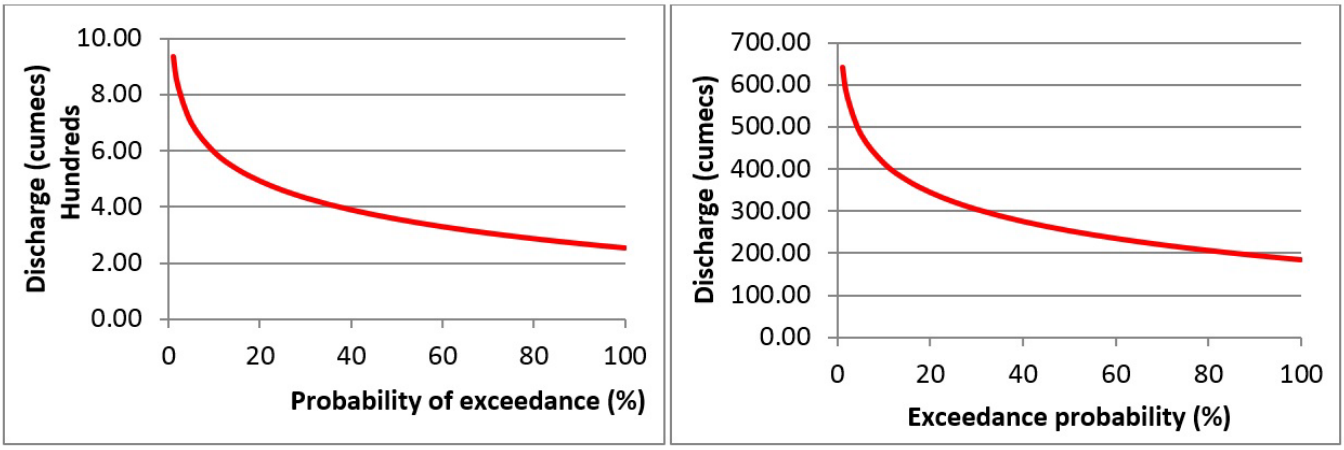

Figure 12: Monthly average flow duration curve for a) 1EE01 (Exponential) b) 1EF01 (Exponential).

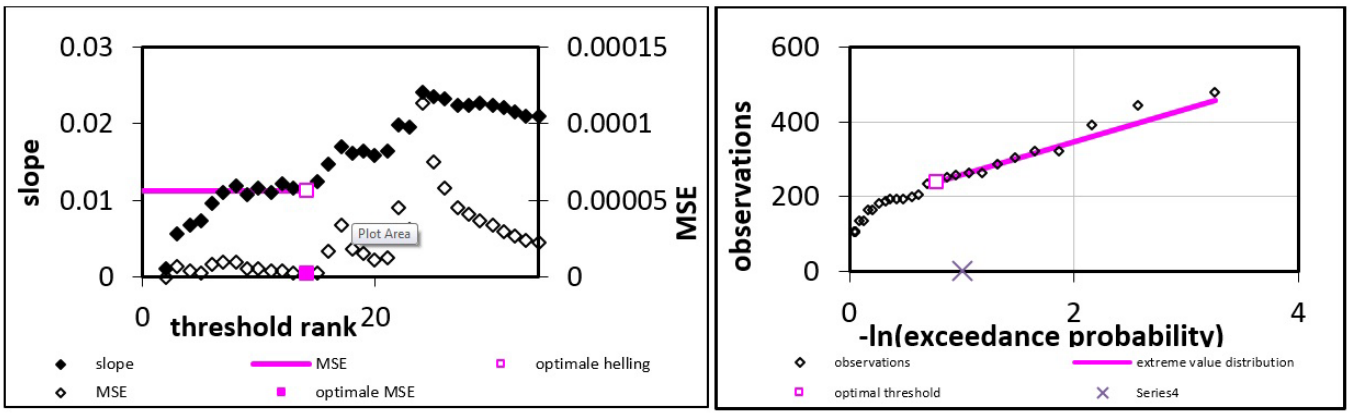

Figure 13: a) Slope exponential Q-Q plot and b) Exponential Q-Q plot for 1EE01.

Using Q80-0.3Q95, where Q80 are estimates for available flow while 0.3Q95 are estimates for environmental flow, it follows that the estimate maximum withdrawal in monthly terms for stations 1EE01 and 1EF01 is 262.5 and 368.4 cumecs respectively.

Low flows analysis: Analyses of low stream flow to indicate the probable availability of water in streams at different return periods the two stations (1EE01 and 1EF01) are presented. Table 12 show a summary of parameters used to generate the Q-Q plot with results. The estimated low flow for different return periods is presented in Table 12 with corresponding graph (Figure 13).

The low flows corresponding to the different exceedance probabilities were also calculated, and the results are shown in the table below and plotted in Figure 14 (Tables 13 and 14).

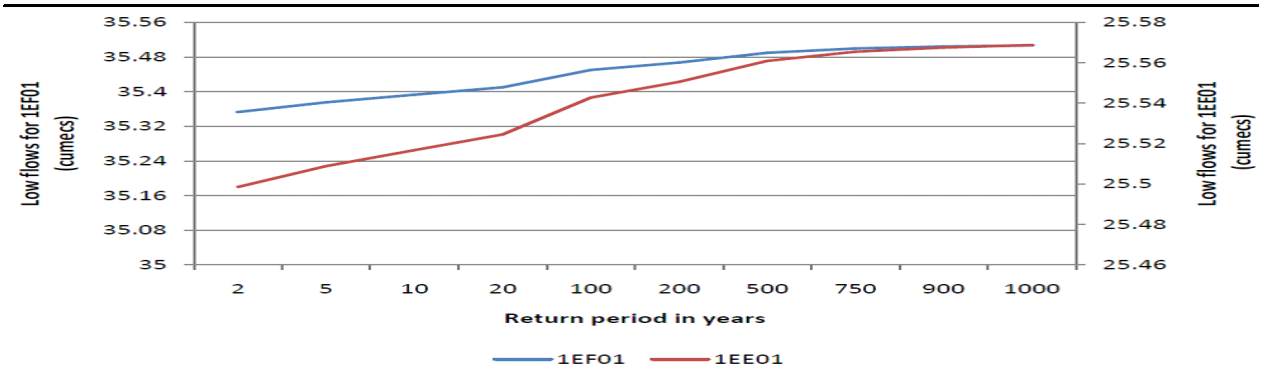

Figure 14: Estimated low flows for different return periods.

Station	Beta	Threshold (X_t)
1EE01	0.0113	0.03923
1EF01	0.0283	0.0248

Table 12: Estimated parameters from Pareto Q-Q plot for 1EE01 and 1EF01 using monthly average flow.

Station	Return period, T (years)									
	2	5	10	20	100	200	500	750	900	1000
1EF01	35.35	35.37	35.39	35.41	35.45	35.47	35.49	35.5	35.5	35.51
1EE01	25.49	25.5	25.51	25.52	25.54	25.55	25.56	25.56	25.56	25.56

Table 13: Estimated low flows for different return periods.

Station	Probabilities of exceedance	Derived using annual minima extracted from daily flows (in cumecs)	Derived using annual minima extracted from monthly average flows (in cumecs)
1EF01	Q80	30.725	45.777
	Q85	28.886	43.054
	Q90	27.252	40.633
	Q95	25.79	38.467
1EE01	Q80	27.377	42.409
	Q85	25.743	39.066
	Q90	24.291	36.095
	Q95	22.991	33.437

Table 14: Exceedance probabilities for monthly and daily averaged low flows, extracted from daily and monthly average flows.

Station	Probabilities of exceedance	Derived using annual minima extracted from daily flows (in cumecs)	Derived using annual minima extracted from monthly average flows (in cumecs)
1EF01	Q80	30.725	45.777
	Q85	28.886	43.054
	Q90	27.252	40.633
	Q95	25.79	38.467
1EE01	Q80	27.377	42.409
	Q85	25.743	39.066
	Q90	24.291	36.095
	Q95	22.991	33.437

Table 15: Summary of Probable Maximum Precipitation for the different stations.

Probable maximum precipitation: Analysis of probable maximum precipitation was based on annual maximum monthly rainfall. The results obtained are summarized in the Table 15.

Conclusion

Mitigating potential severe impacts of hydrological extremes requires understanding of hydrological characteristics at a range of spatio-temporal scales. In this study, data quality control showed consistency in rainfall, temperature and discharge datasets. Observed and generated hydrograph between November 2010 and July 2012 showed that higher flows were simulated with more accuracy than lower flows. However, the maximum runoff values derived from the model at this timescale was not representative since individual floods are caused by episodic rainfall events.

The Maximum and minimum monthly and annual flows and rainfall derived from the generated box plots showed maximum flows centered in the months of March to May (peak rainfall season) with increasing trends in temperature. Graphical plots of observed rainfall showed a slight increasing trend in all stations except Eldoret Soil Conservation Service Station, which had a slight decreasing trend and Bungoma Water Supply which had no trend at all. The trends, seasonality and cycles in the series were identified and maximum values in rainfall and discharge were noted to closely follow the pattern for peak rainfall seasons.

Based on the flow magnitudes and 100-year return period, the upstream station (1EE01) was noted to have lower values compared to downstream station (1EF01) for different assumed distributions. Therefore, the flow magnitude values at the downstream station (1EF01) were assumed to be more reliable compared to upstream station. The results of the Exponential and Pareto distributions for the two locations indicated a normal tail, suggesting that the EV1/Gumbel distribution would be an appropriate statistical distribution to calibrate the AM series for the stations. The best conventional calibration results (considering MOM, MLE and PWM calibration) using the EV1/Gumbel superimposed with the extreme value distribution fitted along with the exponential/Pareto Q-Q plots for comparison. The estimate maximum withdrawal in monthly terms for stations 1EE01 and 1EF01 is 262.5 and 368.4 cumecs respectively. Analyses of low stream flow indicate the probable availability of water in streams at different return periods the two stations (1EE01 and 1EF01). Therefore, the results of extreme values analysis of hydrological characteristic provide required information to estimate the water balance and available water for irrigation.

Acknowledgements

The authors would like to thank the Department of Meteorology, University of Nairobi for providing support during the study, the Kenya Meteorological Department for provision of rainfall datasets and Water Resource and Management Authority for provision of river discharge data used for the study.

References

1. Ministry of Water and Irrigation (MoWI) (2009) Flood Mitigation Strategy.
2. Saji NH, Goswami BN, Vinayachandran PN, Yamagata T (1999) A dipole mode in the tropical Indian Ocean. Nature 401: 360-363.
3. Birkett CM, Murtugudde R, Allan JA (1999) Indian Ocean climate event brings floods to East Africa's lakes and Sudd Marsh. Geophys Res Lett 26: 1031-1034.
4. Ndetei CJ, Opere AO, Mutua FM (2007) Flood frequency analysis in Lake Victoria basin based on tail behaviour of distributions. J Kenya Meteorol Soc 1: 44-54.
5. Cunnane C (1989) Statistical Distributions for Flood Frequency Analysis. World Meteorological Organization, Operational Hydrology Report No 33.
6. Gumbel EJ (1941) The return period of flood flows. Ann Math Statist 12: 163-190.
7. Benson MA (1968) Uniform flood frequency estimating methods for federal agencies. Water Resour Res 4: 891-908.
8. Fiering MB (1967) Streamflow Synthesis. Macmillan, London (Chapter 3).
9. Chow KCA, Watt WE (1994) Practical use of the L-Moments, Stochastic and statistical methods in hydrology and environmental engineering. In: Hipel KW (ed.), Vol 1, Kluwer Academic Publishers Group, Boston, MA, USA, pp: 55-69.
10. Vogel RM, Kroll CN (1989) Low-flow frequency analysis using probability-plot correlation coefficients. J Water Resour Plng Mgmt ASCE 115: 338-357.
11. Delleur JW, Rao AR, Bell JM (1988) Criteria for the determination of minimum streamflows. Tech Rep CE-HSE-88-6, School of Civil Engrg, Purdue University, West Lafayette, Ind.
12. Tasker GD (1989) Regionalization of low flow characteristics using logistic and GLS regression. New directions for surface water modeling. In: Kavvas ML (ed.), IAHS Publication No 181: 323-331.
13. Wandle SW, Randall AD (1993) Effects of surfacial geology, lakes and swamps, and annual water availability on low flows of streams in central New England, and their use in low-flow estimation. US Geological Survey Water Resources Investigation Report 93-4092, Washington, DC.
14. Rumenick RP, Grubbs JW (1996) Methods for estimating low-flow characteristics for ungaged streams in selected areas, northern Florida. US Geological Survey Water Resources Investigation Rep 96-4,124, Washington, DC.
15. Werick B (2000) National Drought Atlas, US Army Corps of Engineers, Institute for Water Resources.
16. Hosking JRM, Wallis JR (1987) Parameter and quantile estimation for the generalized Pareto distribution. Technometrics 29: 339-349.
17. Madsen H, Rasmussen PF, Rosbjerg D (1997) Comparison of annual maximum series and partial duration series methods for modeling extreme hydrologic events. 1. At-site modeling, Water Resour Res 33: 747-757.
18. Mkhandi S, Opere AO, Willems P (2005) Comparison between annual maximum and peaks over threshold models for flood frequency prediction. International conference of UNESCO Flanders FIT FRIEND/Nile project–towards a better cooperation, Sharm-El-Sheikh, Egypt, CD-ROM Proceedings, p: 16.
19. Opere AO, Mkhandi S, Willems P (2006) At Site Flood Frequency Analysis for the Nile Equatorial Basins. Physics and Chemistry of the Earth 31: 919-927.
20. Swenson S, Wahr J (2009) Monitoring the water balance of Lake Victoria, East Africa, from space. J Hydrol 370: 163-176.
21. Ngaina JN, Njoroge JM, Mutua F, Mutai BK, Opere AO (2014) Flood Forecasting over Lower Nzoia Sub-Basin in Kenya. Africa Journal of Physical Sciences 1: 25-31.
22. Srikanthan R, Amirthanathan GE, Kuczera G (2007) Real-time flood forecasting using ensemble Kalman filter. In: Oxley L, Kulasiri D (eds.), MODSIM 2007 International Congress on Modelling and Simulation. Modelling and Simulation Society of Australia and New Zealand, pp: 1789-1795.
23. Li L, Hong Y, Wang JH, Adler RF, Policelli FS (2009) Evaluation of the realtime TRMM-based multi-satellite precipitation analysis for an operational flood prediction system in Nzoia Basin, Lake Victoria, Africa. Nat Hazards 50: 109-123.
24. Khan SI, Adhikari P, Hong Y, Vergara H, Adler R (2011) Hydroclimatology of Lake Victoria region using hydrologic model and satellite remote sensing data. Hydrol Earth Syst Sci 15: 107-117.